Development of scanning transmission ion microscopy computed tomography at Fudan microbeam line

LI Yongqiang[1,2] HABCHI Claire[3] LIU Xue[4] LIU Yiyang[4] SHEN Hao[1,*]

[1]*Deaprtmentof Radiation Oncology Fudan University Shanghai Cancer Center*; *Department of Oncology Shanghai Medical Colloge, Fudan Unversity, Shanghai 200032, China*

[2]*Institute of Modern Physics, Applied Ion Beam Physics Laboratory, Fudan University, Shanghai 200433, China*

[3]*University Bordeaux, CENBG, UMR 5797, F-33170 Gradignan, France*

[4]*Research Center of L aser Fusion, CAEP, Mianyang 621900, China*

Abstract The computed tomography was applied to setting STIM (Scanning Transmission Ion Microscopy) projections recorded at the Fudan Ion Beam Laboratory. In this work, in order to visualize the three-dimensional mass density distribution in several specimens, example for a test structure of hollow gold cyliner was presented together with a detailed description of the developed system, including data reconstruction code (Tomorebuild 2) and image display software (AMIRA®). Future development will allow the particle induced X-ray emission tomography for elemental analysis of micrometer-sized samples.

Key words STIM-CT, TomoRebuild, Density distribution

1 Introduction

During the last years, the particle induced X-ray emission (PIXE) and scanning transmission ion microscopy (STIM) microprobe analysis can produce the two-dimensional distribution of elements or mass density. The analysis methods have the ability to measure all of the elements for total concentration and homogeneity simultaneously. With the help of the computed tomography (CT) technique, the energy loss data in many angles are acquired by rotating the sample. It is possible for STIM to determine the three dimensional distribution of the mass density and shape, or the sample internal structure from a set of projections at different orientations[1]. CT development was mainly driven by medical applications[2]. In 1973, Godfrey Hounsfield presented the first medical scanner by X-rays (later he was awarded the Nobel Prize together with Allan Cormack)[3,4]. Because of the effective detection of the transmitted ions and the inherited low beam current, the STIM-CT method is quantitative and relatively non-destructive, and provides mass normalisation information for accurate elemental concentration determination with PIXE.

Recently, the micron beamline at the Fudan Nuclear Microprobe Laboratory is aimed to develop a micro-tomography system, to provide important three-dimensional information of micrometer-sized samples[5]. The STIM tomography system has been carried out, and will be expanded for PIXE tomography[6]. The STIM-CT has become a versatile analytical technique in materials and life science[7].

In this paper, the system is described, and the STIM-CT characterization of gold cyliner for three-dimensional density is presented, demonstrating its micro-tomography application in the nuclear analysis techniques in China.

2 Experimental

The experiment was carried out at the Fudan Nuclear Microprobe Laboratory with the 3-MeV proton beam. An adjusted rectangle collimator is utilized as a

Supported by Chinese National Science Foundation under the Grant (No.10975034).

* Corresponding author. *E-mail address*: haoshen@fudan.edu.cn

Received date: 2012-09-10

configuration object, another is placed before the triplet quadrupole, and 3.5 m away from the former to prevent scattering. For these test experiments, the beam size in the focal plane is around 1-μm diameter.

A windowless Si-PIN diode (Hamamatsu 1223-01), which has a resolution of 25 keV at full width half-maximum (FWHM), is placed behind the sample holder, and about 6 mm away from the sample[8] to measure the protons residual energy[9] after traversing the sample at 0^o. The detector suffers from damage during the experiment since the protons are implanted into the crystal. As soon as the deviation of the measured proton energy in vacuum decreases, the detector is whirled to expose a fresh region[10]. A sample manipulator based on an *x*-*y*-*z* target (*x*, *y*: ±12.5 mm, *z*: 0–50 mm, step: 5 μm) with a steel needle is utilized as rotation axis, and attached to a PC magnetic rotary drive unit, to correct the specimen position in case it moves out of the center view during specimen rotation at the beginning data acquisition[6]. During the experiments, the projection angle of the tomography axis is performed by a computer controlling precision step motor, which is capable of rotation in minimum step of 0.05^o. The control and data acquisition systems in the microprobe facility are running on a PC under MS Windows 2000. The STIM detector, which is connected to OM1000, converts the analog signal to digital signal. The computer controls the scanning size of 2 mm × 2 mm with the Oxford Microbeams Ltd. The data acquisition and the 3D-scan analysis are fully automated. A schematic diagram of a STIM-CT experiment is shown in Fig.1.

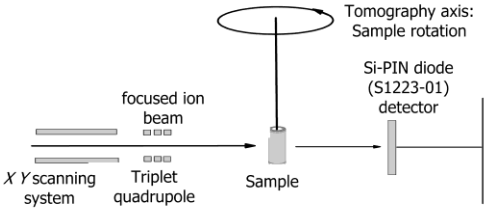

Fig. 1 Schematic diagram of a STIM-CT experiment. The spot size of the incident beam at the specimen surface was adjusted to 2 μm. The proton energy is measured by the Si-PIN dector.

A single and hollow cyliner sample was composed of gold and prepared for the experiment. The non-complex well-characterized structure sample was chosen as a model for STIM-T study due to its regular shape, better column, and concentricity characteristics. The specimens, which were thin enough for transmission of 3 MeV protons, were mounted on top of steel needle using cyanoacrylate adhesive or super glue, dried in air about 12 h, and aligned along the vertical axis.

A 3D-STIM-tomography experiment consists of a number of 2D-STIM sample images, which were called as projections, under different incident angles of $0–180^o$ at the third dimension[11]. The current rate was adjusted to 1000–3000 Hz to avoid any detector damage during the analysis. Under these conditions, the STIM-CT is considered as a non-destructive technique[12]. The transmitted ions are collected by detector, and mechanically whirled at 0^o on the incoming beam axis during the acquisition[13]. The beam scan over the region under study is programmed at the beginning of the experiment. The sample was scanned over the area of 1800 μm ×1800 μm with a total of 128 horizontal slices, and obtained from the 128×128 pixels. The projections were recorded by horizontally scanning the beam over the sample from top to bottom[11]. Several rapid scans for every projection were performed at the speed of the 10 μs/pixel; and the rotation, by a computer controlling precision step motor. A total of 100 projections were recorded over 180^o angular range with 1.8^o steps using the 50 scans/projection. Total duration was about 5 h.

3 TomoRebuild technique

Before data treatment, the experimental tomography data files in Fudan should be converted into the format of Centreď Etudes Nucléaires de Bordeaux Gradignan (CENBG) using specific procedure, and written in Fortran 90®. The TomoRebuild 2 data reduction program was used for data treatment. This code, developed at CENBG, is used to process STIM-CT data before reconstructing 2D or 3D tomography images. Based on the filtered back projection algorithm, the reconstruction is the most popular and the least time-consuming technique for the ideal data [14]. However, the reconstructed image may drastically deteriorate due to noise and misalignment problems in the raw data[6]. How the TomoRebuild software operates can be found in Refs.[13,15].

The graphic software AMIRA® was used to display the 3D structure image of the sample by associating a colour code with density values. The lowest density regions are vacuum characteristic surrounding the sample[16,17].

The specimen outer surface was given according to threshold near low values. Several cutting planes are selected to vision internal structure at any orientation. Automatic calculations are carried out on selected materials to determine thickness, volume and average density of sample.

4 Results and Discussion

Figure 2 shows that the 3D structure of target was reconstructed, and two iso-surfaces are displayed.

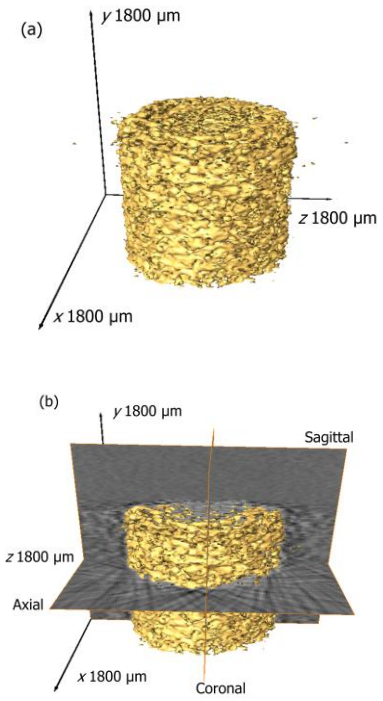

Fig.2 (a) 3D-reconstruction of the reference sample, (b) Position of the three selected slices at three orientations within the reconstructed volume.

The reconstruction of the corrected sonograms for hollow cylinder is shown in Fig.3. The density closed to zero is the limit characteristic between the sample and the surrounding vacuum. The highest densities show the target wall (white), thus distinguishing the gold wall and the interior hollow. The picture is strongly affected by artefacts represented as streaks outside the sample region. These artefacts originate from the insufficient number of projection angles in combination with the mean filtering of the energy loss values[18].

The result shows there are many deviations from the ideal projection process[19]. The experimental conditions affect getting an approximation closer to the ideal projection process. The specific ion beam characteristics are concerned. (1) The energy dependence on the stopping power should be considered[10]. Described by the linear stopping power, the energy loss of ion passing through a specimen is related to the incident beam energy, and converted to the projected areal mass density along this trajectory, prior to the reconstruction of the stopping power[20].

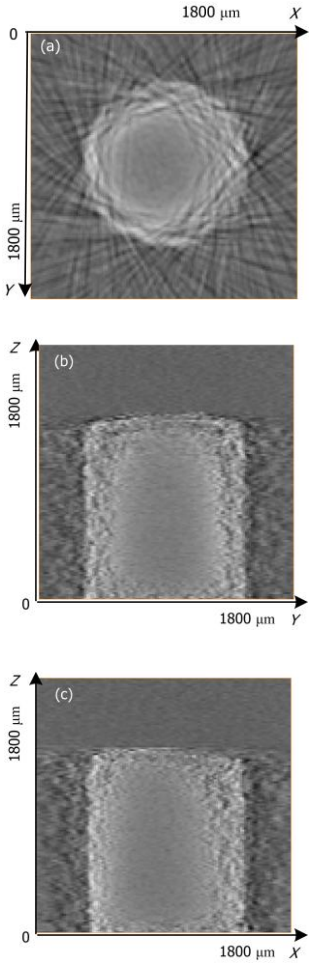

Fig.3 The reconstructed ion microtomography slice of target from three orientations. (a) Axial orientation, (b) coronal orientation, and (c) sagittal orientation.

(2) The beam broadening within the specimen (lateral straggling) should be considered[21]. The resulting beam profile, that defines the interaction volume within the specimen, is a convolution of the incident beam profile, and the broadening function due

to the multiple scattering with the electrons in the specimen. It is important that the interaction volumes for each ion trajectory do not overlap. Otherwise, the spatial resolution of the reconstructed specimen is degraded. For a given specimen, the incident energy and the specimen thickness control the broadening of the proton beam[10]. A further effect, which is caused by the statistical nature of the multiple interactions between the ions and the electrons of the material, is energy straggling. After interacting with the matter[22,23], a beam of defined energy has a Gaussian energy distribution.

Figure 4 presents the possibility of stacking the reconstructed slices and performing three-dimensional tomography. An artificial cut was conducted along the symmetry axis, to illustrate the object shape and its internal structure[6].

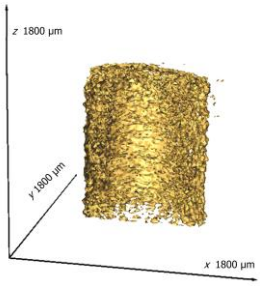

Fig.4 Target 3D image. An artificial cut along the symmetry axis illustrates the internal structure and the target wall surface.

5 Conclusion

This study on hollow cyliner sample can perform 3D STIM-CT experiment setup in the micron beamline at the Fudan Nuclear Microprobe Laboratory. The more accurate quantitative STIM tomography and the rotation axis alignment with higher precision will be performed. Further, the PIXE-T information will be conducted to characterize the elemental distributions within the sample and obtain a more accurate quantitative mass density determination.

Acknowledgements

The authors thank accelerator group for good beam condition during experiments.

References

1 Kak A C. Principles of computerized tomographic imaging, New York (USA), IEEE Press, 1987, 50–60.

2 Cormack A M, Koehler A M. Phys Med Biol, 1976, **21:** 560–569.

3 Shampo M A, Kyle R A. Mayo Clin Proc, 1996, **71:** 990–996.

4 Bautz W, Kalender W, Godfrey N. Radiologe, 2005, **45:** 350–355.

5 Zhang C H, Li M, Hou Q, Nucl Sci Tech, 2011, **22:** 89–94.

6 Wegdén M, Elfman M, Kristiansson P, *et al*. Nucl Instrum Meth B, 2006, **249:** 756–759.

7 Liu C, Gu W G, Qian N, *et al*. Nucl Sci Tech, 2012, **23:** 277–283.

8 Li Y Q, Satoh T, Shen H, *et al*. Nucl Sci Tech, 2011, **22:** 282–286.

9 Liu J F, Bao L M, Yue W S, *et al*. High Power Laser Part Beam, 2008, **20:** 313–318.

10 Michael S, Arthur S, Tilo R, *et al*. Ultramicroscopy, 2006, **106:** 574–581.

11 Reinert T, Sakellariou A , Schwertner M, *et al*. Nucl Instrum Meth B, 2002, **190:** 266–270.

12 Xia Y, Ma T Y, Liu Y Q, *et al.* Nucl Sci Tech, 2011, **22:** 144–150.

13 Gordillo N, Habchi C, Daudin L, *et al*. Nucl Instrum Meth B, 2011, **269:** 2206–2209.

14 Bench G, Nugent K A, Cholewa M, *et al*. Nucl Instrum Meth B, 1991, **54:** 390

15 Michelet H C, Incerti S, Aguer P, *et al*. Nucl Instrum Meth B, 2005, **231:** 142–148.

16 Zhang X Z, Qi Y J, Nucl Sci Tech, 2011, **22:** 338–343.

17 Dai T T, Ma T Y, Liu H, *et al.* Nucl Sci Tech, 2011, **22:** 344–348.

18 Cheng Y, Tuo X G, Huang L M, *et al.* Nucl Sci Tech, 2011, **22:** 151-155.

19 Jiang Y J, Cui Y, Huo Y Z, *et al.* Nucl Sci Tech, 2011, **22:** 185–192.

20 Pontau A, Antolak A J, Morse D H, *et al*. Nucl Instrum Meth B, 1989, **40/41:** 646–650.

21 Antolak A J. Nucl Instrum Meth B, 1988, **30:** 182–184.

22 Michelet C, Ph. Moretto, Laurent G, *et al*. Nucl Instrum Meth B, 2001, **181:** 157–163.

23 Breese M, Jamieson D N, King P. Materials Analysis using Nuclear Microprobes, New York (USA): Wiley press, 1996, 102.